Taylor & Francis
Taylor & Francis Group

Philosophical Magazine

ISSN: 1478-6435 (Print) 1478-6443 (Online) Journal homepage: https://www.tandfonline.com/loi/tphm20

# Amorphous boron nitride at high pressure

Murat Durandurdu

**To cite this article:** Murat Durandurdu (2016) Amorphous boron nitride at high pressure, Philosophical Magazine, 96:18, 1950-1964, DOI: 10.1080/14786435.2016.1183830

**To link to this article:** https://doi.org/10.1080/14786435.2016.1183830

PHILOSOPHICAL MAGAZINE, 2016
VOL. 96, NO. 18, 1950–1964
http://dx.doi.org/10.1080/14786435.2016.1183830

Taylor & Francis
Taylor & Francis Group

# Amorphous boron nitride at high pressure

Murat Durandurdu

Department of Materials Science & Nanotechnology Engineering, Abdullah Gül University, Kayseri, Turkey

**ABSTRACT**

The pressure-induced phase transformation in hexagonal boron nitrite and amorphous boron nitrite is studied using *ab initio* molecular dynamics simulations. The hexagonal-to-wurtzite phase transformation is successfully reproduced in the simulation with a transformation mechanism similar to one suggested in experiment. Amorphous boron nitrite, on the other hand, gradually transforms to a high-density amorphous phase with the application of pressure. This phase transformation is irreversible because a densified amorphous state having both $sp^3$ and $sp^2$ bonds is recovered upon pressure release. The high-density amorphous state mainly consists of $sp^3$ bonds and its local structure is quite similar to recently proposed intermediate boron nitrite phases, in particular tetragonal structure ($P4_2/mnm$), rather than the known the wurtzite or cubic boron nitrite due to the existence of four membered rings and edge sharing connectivity. On the basis of this finding we propose that amorphous boron nitrite might be best candidate as a starting structure to synthesize the intermediate phase(s) at high pressure and temperature (probably below 800 °C) conditions.

**ARTICLE HISTORY**
Received 14 March 2016
Accepted 23 April 2016

**KEYWORDS**
Polyamorphism; boron nitride; amorphous; phase transformation

## 1. Introduction

Boron nitride (BN) is one of important ceramics with considerable current interest because of its superior optical, electrical and mechanical properties. BN has four crystal forms. The hexagonal phase ($P6_3/mmc$) (*h*-BN) [1], analogous to graphite, is known as the most stable form of BN, which has a two-dimensional (2D) layered structure consisting of $sp^2$ bonds. Similar to *h*-BN, rhombohedral BN (*r*-BN) has a layered structure as well [2]. The layers of BN in both phases are identical but their stacking sequences are different. The interlayer separations in these 2D crystals are quite large and thus their density is low. Consequently they sometimes can be referred as low-density phases of BN. Due to this feature, these crystals can be easily compressible under external stresses. BN has two three-dimensional (3D) modifications that are tetrahedrally coordinated the zinc-blende structure having $F\bar{4}3m$ symmetry (*c*-BN) and wurtzite structure with $P6_3mc$ symmetry (*w*-BN) consisting of $sp^3$ bonds [3,4]. Both structures are easily synthesized at high temperature and pressure conditions from *h*-BN or *r*-BN [3–19]. The *h*-BN → *w*-BN and *r*-BN → *c*-BN phase changes

**CONTACT** Murat Durandurdu murat.durandurdu@agu.edu.tr

are displacive type phase transformations while the *h*-BN → *c*-BN transformation is a reconstructive one in which bond breaking occurs. The phase transition into *c*-BN or *w*-BN has been attracted many attentions. Temperature and the properties of initial samples appear to have large influences on the high-pressure behavior of these systems and they can lead to substantially different transformation pressures and mechanisms [3–19].

There have been significant investigations to understand the transformation mechanism of these simple phase transitions and to predict stable novel allotropes of BN that might possess superior properties with some high-tech potential applications as in the other forms of BN. To date these investigations have proposed several intermediate phases for the *h*-BN → *w*-BN phase transformation: orthorhombic structures (O-BN) with the *Pbam* (Z-BN with the structure of Z-carbon) [20] and the $Pmn2_1$ space group [21], and a tetragonal phase within $P4_2/mnm$ symmetry (analog of the bct carbon) [22]. All these phases are a potential candidate for superhard materials like *c*-BN and *w*-BN but to our knowledge, they have not been synthesized in any experiments yet.

Considering electronic structure of BN polymorphs discussed above, they all possess semiconducting properties with different band gap energy [23]. However a metallic tetrahedral structure with $P\bar{4}m2$ space group has been recently proposed in first principles simulations [23].

Contrary to extensive researches on the crystalline BN phases under pressure, investigations on another fascinating forms of BN, amorphous BN (*a*-BN), and turbostratic BN (*t*-BN) at high-pressure and temperature conditions are limited [24–32]. Although the equation of state of *t*-BN under static high-pressure compression was discussed in Ref. [28] up to 6.1 GPa, to our knowledge no pressure-induced phase transformation has been reported for *t*-BN at room temperature yet. At 20 GPa and 1770 K, on the other hand, *t*-BN transformed to the high-purity bulk nanostructured *c*-BN (grain size ~20 nm) [29]. Nanostructured *c*-BN formed in the *t*-BN domains via a mechanism having both the pressure-induced buckling of layers and change of the mutual orientation of layers [30,31] and exhibited superior properties such as excellent wear resistance, fracture toughness and extremely high hardness relative to microcrystalline *c*-BN. In a shock compression experiment [32], a phase transformation from *t*-BN to *c*-BN was detected. It was reported that temperature and the degree of the turbostratic disorder of the starting structures played important roles in promoting *t*-BN-to-*c*-BN phase transformation [32].

For the case of *a*-BN experiments mostly focused on its crystallization at low-pressure regimes and high temperatures (800 °C and higher) and reported its transformation into *c*-BN, *w*-BN or *h*-BN depending on the topology of initial samples (degree of disorder) and temperature applied [24–27]. The main purpose of some of these experiments was indeed to produce the 3D crystalline BN phases and to reduce the thermodynamic conditions for the $sp^2 \rightarrow sp^3$ phase transitions using some catalysis or solvents [24–27]. To our knowledge a pressure-induced amorphous-to-amorphous phase transition in BN, a phenomenon observed in some disordered materials including metallic glasses [33,34], has not been reported in the Literature so far. Since the crystalline BN phases having $sp^3$ bonds are particular interest due to their outstanding mechanical properties, the observation of a quenchable high-density amorphous (HDA) state consisting of $sp^3$ bonds might lead to a new direction in BN studies.

The primary objective of the present work is to explore the response of *a*-BN to the high-pressure using a constant pressure *ab initio* technique. In order to reach our goal, we

investigate not only *a*-BN but also *h*-BN under pressure. The *h*-BN → *w*-BN is successfully observed in the simulation with a transformation mechanism similar to one reported in experiment. For *a*-BN, we propose a phase transformation from a low-density amorphous (LDA) phase to a HDA phase having mostly $sp^3$ bonds. The HDA phase is found to be topologically similar to the intermediate phases, specifically the tetragonal bct type, due to the presence of four membered rings and dominated edge-sharing connectivity. The LDA → HDA transformation progresses gradually and upon pressure release neither the original nor the HDA phases are recovered and instead a mixture state having both HDA and LDA configurations is achieved.

## 2. Methodology

An *ab initio* code, SIESTA [35], based upon the density functional theory (DFT), was selected to perform the MD simulations. This *ab initio* technique was successfully applied to generate a 216 atoms model of *a*-BN from the liquid state [36]. The *a*-BN model is almost chemically ordered and has dominated $sp^2$ bonding that leads to predominantly hexagonal rings as in the most stable boron nitrite phase. The model also has a small amount of $sp^3$ bonding. All these findings seem to agree well with experiments [37,38]. To study the high-pressure behavior of *a*-BN, the simulation parameters of Ref. [36] were adopted. The norm-conserving pseudopotentials [39] were contracted using the Troullier and Martins scheme. The Becke gradient exchange functional [40] and Lee, Yang, Parr correlation functional [41] were used to estimate the exchange correlation energy. The double zeta plus polarized basis sets were implemented. The Brillouin zone integration was performed using solely Γ point. The isoenthalpic-isobaric ensemble (NPH) was chosen to execute the MD simulations. The Parrinello–Rahman method [42] implemented in the SIESTA code was selected to apply pressure. The external pressure was raised progressively by an increment of 5 GPa at low-pressure regimes and of 10 GPa at high-pressure regimes. A period of 7000 MD steps was found to be sufficient to have a relaxed configuration at each applied pressure. The time step of each MD simulation was chosen to be one femtosecond. During the simulations, the power quenching technique [43–45] was adopted, in which the velocity components for atoms and simulation box were set to zero when the velocities and forces had opposite signs. The main reason for choosing this technique was to have an optimized structure at each applied pressure. For *h*-BN, we used a 72-atom supercell. For the energy-volume calculation of the unitcells of *h*-BN and *w*-BN, a variable cell optimization technique was used to relax them till the maximum force is less than 0.01 eV/Å. The Brillouin zone integration was carried out with 10 × 10 × 8 k-point mesh for the *h*-BN and *w*-BN phases via the Monkhorst and Pack method [46]. We used the ISAACS [47] and VESTA [48] programs to analyze the amorphous and crystalline structures.

## 3. Results

### 3.1. Hexagonal BN under pressure

Although the simulation technique and the parameters (basis, pseudopotentials etc.) produce reliable results for *a*-BN, we first study the pressure-induced phase transition of *h*-BN to confirm that they are reliable enough to capture its high-pressure behavior as well. The

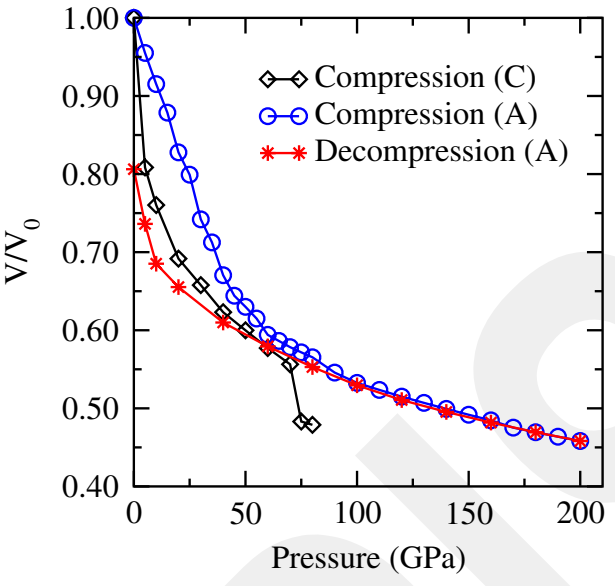


**Figure 1.** (colour online) Pressure–volume relation of *h*-BN on compression and *a*-BN on compression and decompression.

pressure-volume relation of *h*-BN is given in Figure 1. The variation of volume is drastic as expected and due to the open structure (layered) of *h*-BN. At 75 GPa, the volume suddenly declines, suggesting a first order phase transition. An analysis of the structure implies that *h*-BN converts to a *w*-BN phase (Figure 2), agreeing with experiments. Yet the transition pressure predicted in the simulation is about a factor of about 5–9 higher than the experimental critical pressures of ~8–14 GPa [4,6,9,13]. Indeed an overestimated critical pressure is a major shortcoming of the Parrinello–Rahman technique and is correlated to simulation conditions, for example, lack of surface effects due to the use of periodic boundary conditions, the use of ideal structure, fast pressurizing etc. Yet we can estimate a critical pressure for *h*-BN → *w*-BN from the thermodynamic theorem. Both phases are studied at different volumes ($V$) and corresponding internal energies ($E$) are estimated. Then the enthalpy ($H = E + PV$) is calculated. The enthalpy curve of *h*-BN and *w*-BN given in Figure 3 crosses at ~11 GPa, indicating a phase transition at this pressure. The predicted critical pressure from the thermodynamic criterion is in the range of with the experimental results of ~8–14 GPa [4,6,9,13].

Based on the variation of simulation cell vectors at 75 GPa, we can speculate a transformation mechanism for the *h*-BN → *w*-BN phase change. Figure 4 shows the modification of lengths and angles of the supercell as a function of MD simulation time step. The structure is drastically compressed along the *c*-direction while it shows almost no alteration along the other axes. Furthermore the cell angles remain almost null, indicating that the phase transformation does not engage any shear deformation. The mechanism observed in the present study is indeed parallel to what has been proposed in experiment [13].

All these findings provide strong evidence that the simulation technique and parameters are reliable at high pressure as well and hence they can be safely applied for the investigation of *a*-BN under pressure.

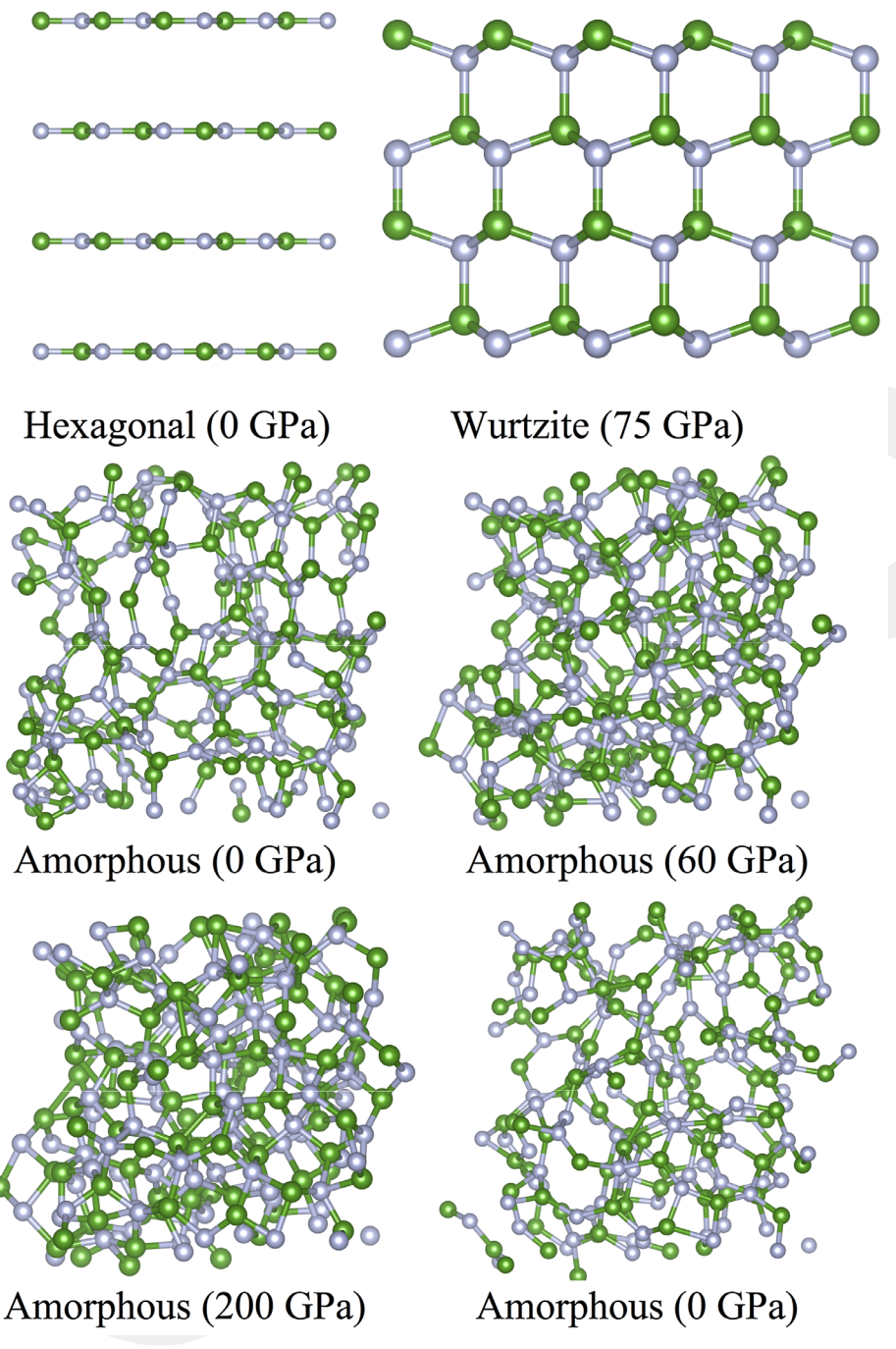


**Figure 2.** (colour online) Ball and stick representation of amorphous and crystalline forms of BN. Dark (green) and light (gray) spheres are B and N atoms, respectively.

### 3.2. Amorphous BN under pressure

The initial amorphous model with some hexagonal nanosheets is compressed until its density is roughly equal to that of *w*-BN observed at 75 GPa in our simulation. The equation

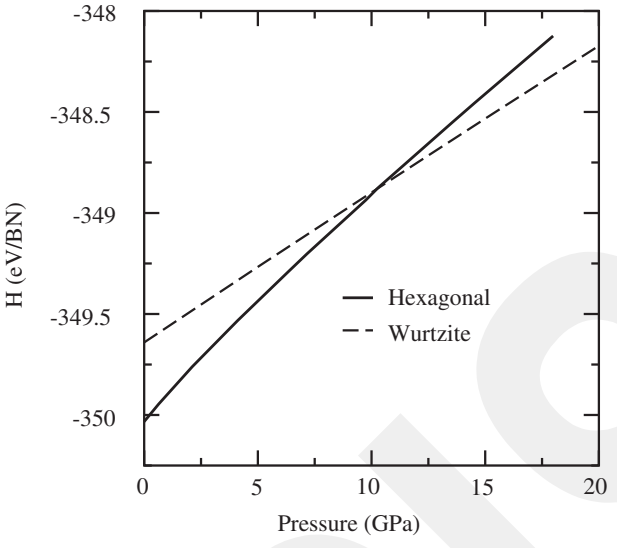


**Figure 3.** Enthalpy curves of the *h*-BN and *w*-BN structures.

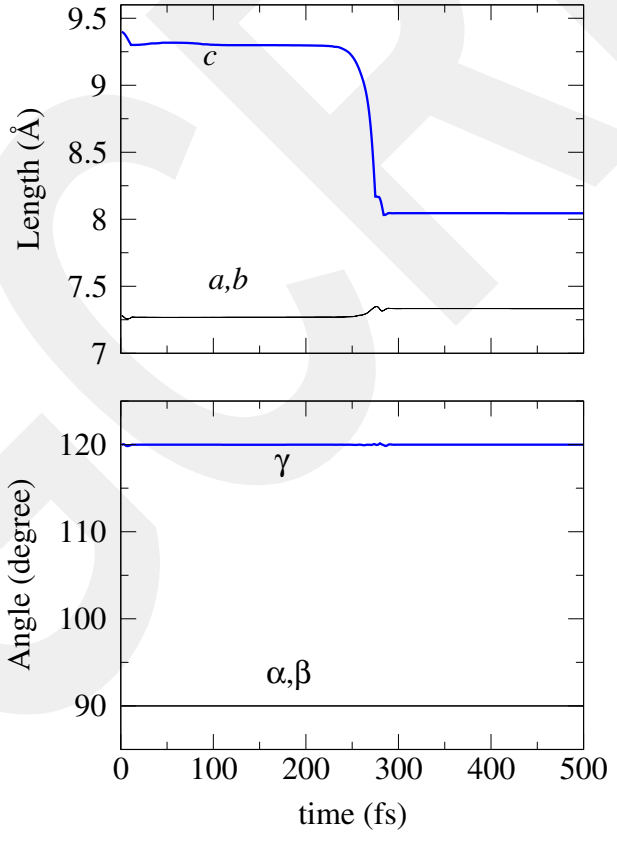


**Figure 4.** (colour online) Simulation cell lengths and angles as function of MD time step.

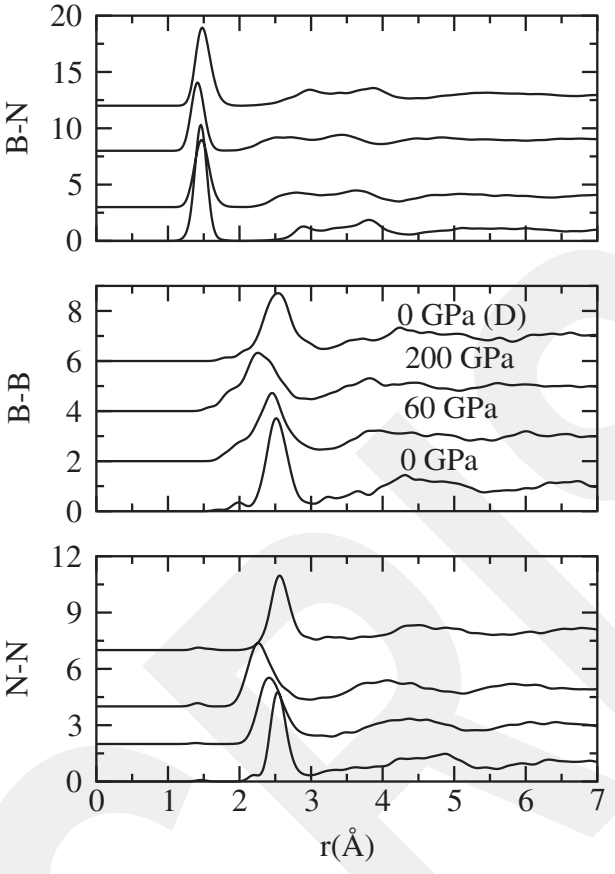


**Figure 5.** Partial pair distribution functions (PPDFs) at selected pressures.

of state of *a*-BN is also provided in Figure 1. As understood from the figure, the volume decreases quickly up to 60 GPa. The pressure–volume curve then presents a change in slope and the decrease in the volume becomes slower. The change in the slope signifies a possible phase transition in *a*-BN. The modification of volume is generally smooth except some ripples at several pressures below 60 GPa, which is probably associated with the finite size of the system. Based upon the variation of the volume and coordination number (see below), the pressure-induced phase change in *a*-BN is interpreted as a continuous transformation. Upon pressure release, the path followed from 200 GPa is reversed up to 60 GPa. After this pressure, the curve develops a hysteresis and the initial density and structure are not recovered. These observations imply that pressure leads to a permanent densification in *a*-BN by possibly removing the free volume of the amorphous network and/or inducing irreversible higher coordinated configurations.

The partial pair distribution functions (PPDFs) given in Figure 5 indicate that the model remains amorphous at 200 GPa (Figure 2). This observation provides first evidence for an amorphous-to-amorphous phase transition in BN. In order to see how the LDA–HDA phase transformation is locally evoked, the structure at each applied pressure is carefully analyzed by the PPDFs. At ambient condition the first neighbor B–N separation is located

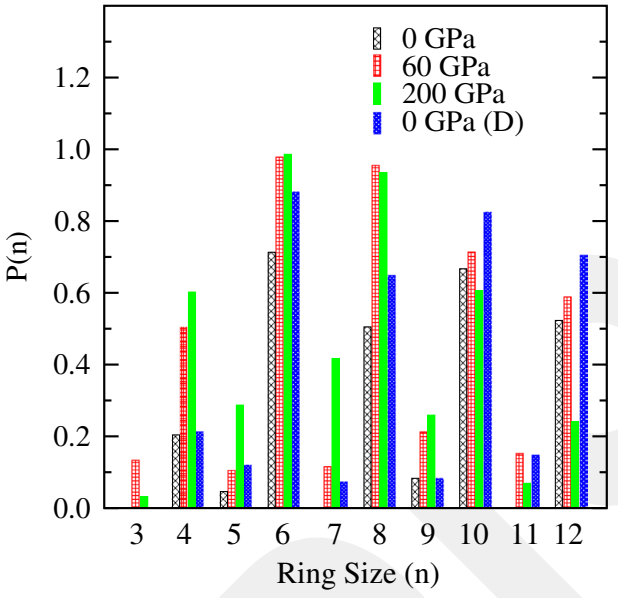


**Figure 6.** (colour online) Ring distribution at selected pressures.

at 1.46 Å, which is indeed close to the B–N bond distance of 1.44 Å formed in *h*-BN [49]. The position of the main B–B (2.51 Å) and N–N (2.54 Å) peaks are also comparable with the second neighbor (B–B or N–N) separations of 2.50 Å for *h*-BN [49]. The weak peak at 1.47 Å in the N–N pair and 1.70 Å in the B–B pair are the indication of homopolar bonds in the network but their frequency is negligible small. Only 0.62% of B and N atoms involve the chemical disorder. The shoulder in the N–N (~2.2 Å) and B–B (~ 2.01 Å) distributions is due to the four membered BN rings (see Figure 6), similar to ones formed in BN nanocages [50,51]. With the application of pressure, the B–N bond distance exhibits a complex behavior with some fluctuations as illustrated in Figure 7: it decreases at the beginning and then has a tendency to increase between 25 and 60 GPa. It starts to decrease again after 60 GPa. The peaks of the N–N and B–B correlations, on the other hand, shift toward lower distances and their main peak is broadened due to the formation of more four membered rings under pressure as shown Figure 6. Pressure does slightly change the number of homopolar bonds, resulting into more odd membered rings in the system (see Figure 6). N and B atoms present 2.39 and 2.85% wrong bonds at 200 GPa, respectively and some of which persist in the network on pressure release. 1.72% B and N atoms are found to involve wrong bonds in the quenched state at zero pressure.

The pressure-induced phase transitions in disordered insulating or semiconducting systems are commonly recognized by the coordination modification. The variation of average coordination number (CN) of *a*-BN upon compression and decompression is given in Figure 8. At zero-pressure, the average CN is 2.97 and is unaffected up to 20 GPa, indicating a tighter packing of the amorphous network without undergoing significant structural rearrangements. After this pressure, the CN increases severely up to 60 GPa, then slowly and reaches a constant value of ~3.85 beyond 170 GPa. Upon pressure release, the CN initially decreases deliberately to a value of ~3.62 up to 20 GPa and then it quickly declines to ~3.20 at zero pressure. This finding offers supportive evidence for an irreversible phase

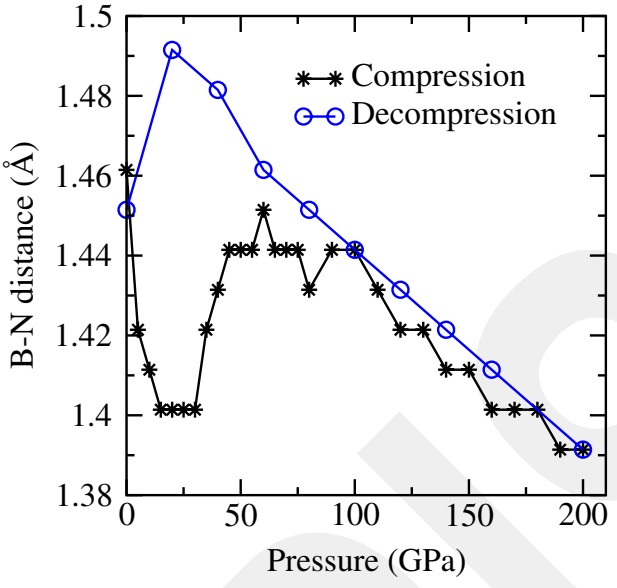


**Figure 7.** (colour online) Variation of B–N bond distance during compression and decompression of *a*-BN.

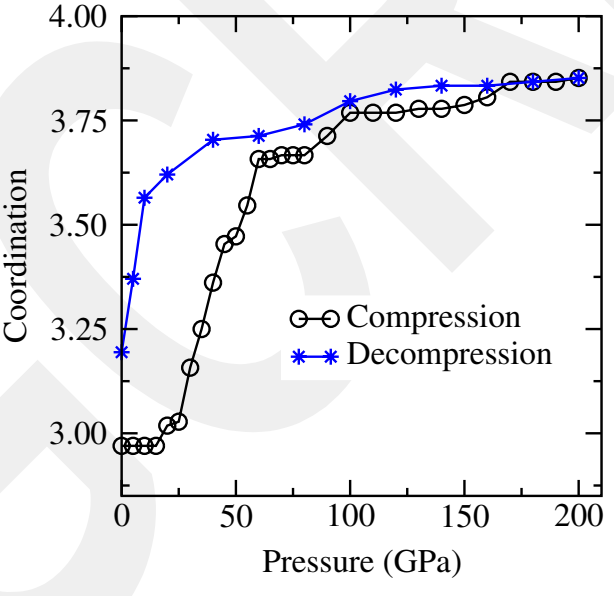


**Figure 8.** (colour online) Modification of coordination number upon compression and decompression of *a*-BN.

transformation in *a*-BN. The distribution of CN at several pressures shown Figure 9 can provide supplementary information about the microstructure of the amorphous system. At zero pressure, 91% of atoms are threefold coordinated and the rest are twofold (6%) and fourfold (3%) coordinated. At 200 GPa, the fraction of fivefold, fourfold, threefold coordination is ~2, 85 and 13%, respectively. The amorphous model obtained on the decompression

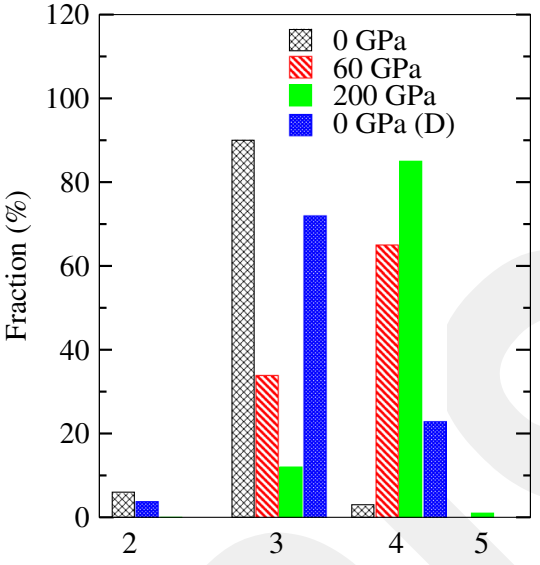


**Figure 9.** (colour online) Coordination distribution at selected pressures.

has predominantly threefold coordination (72%) and a non-negligible amount of fourfold coordination (24%). This means that some of $sp^3$ bonds persist in the amorphous system upon decompression.

To have additional information about the structural rearrangements due to the applied pressure, we also study the bond angle distribution functions (BADFs) of *a*-BN. Its B–N–B and N–B–N angle distributions at particular pressures are illustrated in Figure 10. The model has very broad distributions with the main peak located around 120° as in h-BN. The tetragonal rings produce the subpeak around 80° and 95° in the B–N–B and the N–B–N distributions, respectively while the chain-like structures yield the angles larger than 130°. After 25 GPa, the main peak in the both distributions gradually shift to lower angles and at ~60 GPa, the main peak is located at around of 109°, indicating tetrahedral configurations. The peaks at around 80–90° still persist at 60 GPa and even at 200 GPa, they are broadened and their intensity is increased, indicating that the formation of more tetrahedral rings with the application of pressure (see Figure 6). It should be pointed out here neither *c*-BN nor *w*-BN presents four membered rings but almost all intermediate phases proposed based on *ab initio* investigations have four membered rings and the bond angles ranging from ~85° to ~118°, similar to ones observed in the HDA phase. Therefore the HDA phase might carry some characteristics of the intermediate phase(s). The amorphous model obtained on decompression has a main peak at 120° for the N–B–N distribution and 114° for the B–N–B distribution. Also note that the intensity of peaks due to the four membered rings is slightly higher relative to that of the original network because some four membered rings persevere on pressure release.

Finally the electronic density of states (EDOS) is used to predict the impact of pressure on the electronic structure. To calculate the EDOS, the structure at several pressures is relaxed using a criterion of 0.01 eV/Å for the maximum force. The computed EDOSs are illustrated in Figure 11. As seen from the figure, the pressure-induced metallization does not occur

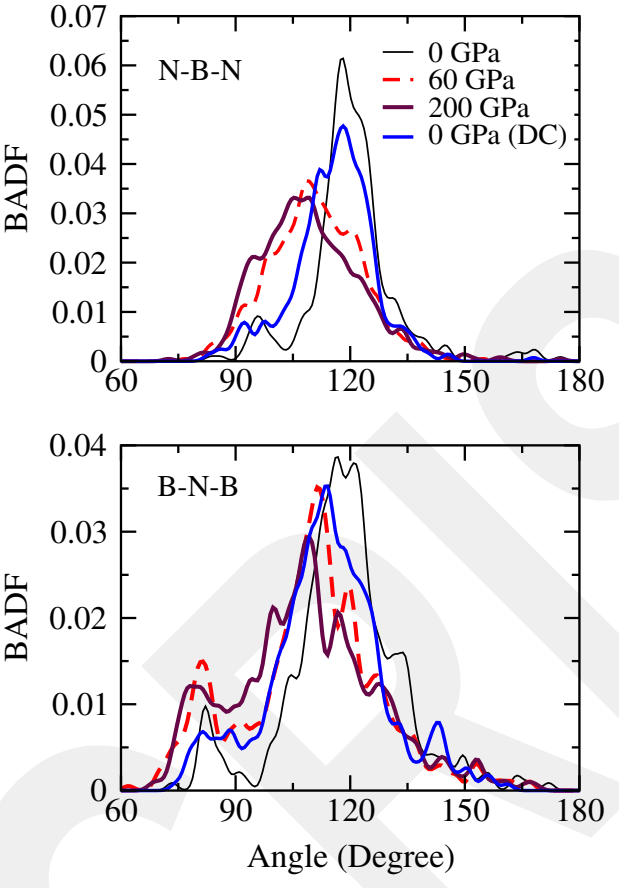


**Figure 10.** (colour online) BADFs at selected pressures. DC: decompression.

in the amorphous form of BN although some midgap states are presented between 60 and 170 GPa. This observation might be not astonishing because all crystalline BN phases are a semiconductor except the O-BN phase having the $P\bar{4}m2$ space group [23].

## 4. Discussion

From the pressure–volume relation (Figure 1), it can be seen that *h*-BN is more compressible than *a*-BN. This behavior is attributed to the dimensionality of these structures. *a*-BN has randomly distributed hexagonal-like nanoscale configurations and some of which are bended or connected via chainlike structures. Furthermore these nanostructures are not stacked in the same direction (a lack of order for directions) unlike *h*-BN. Therefore *a*-BN has neither 2D nor 3D structures but their mixture. So the mix state (2D + 3D) exhibits more resistivity to pressure than the 2D *h*-BN phase.

The amorphous-to-amorphous phase transformation can be first order or continues. Here the origin of continues amorphous-to-amorphous phase transition of *a*-BN is again attributed to the topology of *a*-BN. As mentioned above, *a*-BN is a mix state of 3D and 2D configurations with a non-uniform coordination distribution (differently bonded domains)

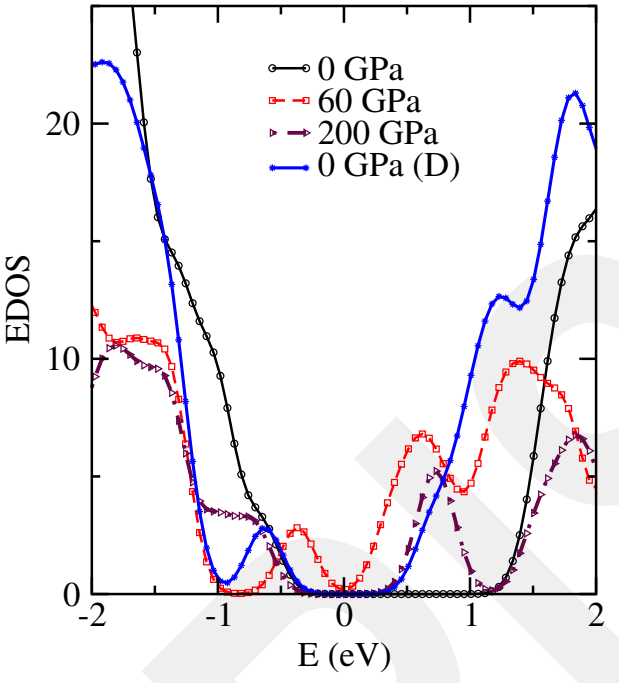


**Figure 11.** (colour online) EDOS near the band gap at selected pressures.

and has randomly distributed voids. Therefore under pressure, the stress distribution is expected to be inhomogeneous in the model, i.e., the local stress alters from place to place. Due to this feature, some portions of *a*-BN are anticipated to be more squeezable than the other portions, which promote random nucleation and coordination modification in the model.

Four membered rings as seen in BN nanocages exist in *a*-BN and more develop with the application of pressure, which yields a structure having dominated edge sharing connectivity. The HDA phase at 200 GPa shows 83% edge sharing tetrahedra and 17% corner sharing tetrahedra. Since both *c*-BN and *w*-BN are assembled by only corner sharing tetrahedra, the HDA phase differs locally from them. On the other hand, the intermediate phases (orthorhombic and tetragonal) predicted based on the *ab initio* calculations consist of edge sharing tetrahedra. In the tetragonal bct-like phase, the connectivity is due to only edge sharing tetrahedra while in the other phases the connectivity is as a result of both edge sharing and corner sharing tetrahedra. Indeed based on the connectivity of the model, it is not easy to have a clear conclusion on the local structure of the HDA phase but the dominated edge sharing tetrahedra in the HDA might provide some evidence that its short-range order is close to the bct-like phase. Yet the existence of corner sharing tetrahedra suggests that the HDA phase also carry some signatures of the orthorhombic, *w*-BN or *c*-BN phases.

Starting from an amorphous structure, the observation of a HDA phase similar to the intermediate phase(s) is particularly important because it provides supportive evidence for their existence in BN. Also on the basis of our findings here we propose that *a*-BN can be used as a starting structure to produce the intermediate phase(s). Yet the application

of high temperature along with pressure is necessary for the reconstructive amorphous-to-crystalline intermediate phase transformation. Temperature should be less than 800 °C because the temperature above 800 °C leads to *c*-BN.

One can question that the predicted amorphous-to-amorphous phase transformation in *a*-BN is due to the limitations of the simulations such as fast pressurizing, the finite size of the model etc. We suspect that this possibility is remote since the Parrinello–Rahman method implemented in the SIESTA code is very successful in producing an amorphous-to-crystalline phase transformation in AlN, As and complex metallic glasses. Yet as mentioned above, the exaggerated critical pressure is anticipated in the simulations. Therefore, the modification of the coordination in *a*-BN is expected to take place at low pressures in experiments. Based on the observation of the critical pressure predicted for the *h*-BN → *w*-BN phase transformation in the Parrinello–Rahman simulation and thermodynamic theorem, the pressure at which coordination starts to increase in *a*-BN is roughly estimated to be ~2.7–5 GPa.

## 5. Conclusions

The high-pressure behavior of *h*-BN and *a*-BN is studied by means of *ab initio* MD simulations. The *ab initio* technique successfully reproduces the *h*-BN → *w*-BN phase transformation. The *h*-BN → *w*-BN phase transformation is due to the compression of *c*-axis as observed in experiment [13]. For the first time an amorphous-to-amorphous phase transformation is proposed for BN. This is an irreversible gradual phase transformation since pressure leads to a permanent densified amorphous state with $sp^3$ and $sp^2$ bonds. The HDA state is predominantly fourfold coordinated and found to be topologically close to the intermediate tetragonal bct-like phase rather than the known *w*-BN or *c*-BN due to the presence of edge sharing tetrahedra. Based on our observations, we suggest that the amorphous form of BN might be best chose as an initial structure to synthesize the intermediate phase(s) with the application of temperature (below 800 °C) along with pressure. The electronic structure calculations reveal that the metallization does not occur in *a*-BN under pressure.

## Acknowledgement

The calculations were partially run on TÜBİTAK ULAKBİM, High Performance and Grid Computing Center (TRUBA resources).

## Funding

This work was supported by the Scientific and Technical Research Council of Turkey (TÜBİTAK) [grant number 114C100].

## References

[1] R.T. Paine and C.K. Narula, *Synthetic routes to boron nitride*, Chem. Rev. 90 (1990), pp. 73–91.
[2] Y. Matsui, Y. Sekikawa, T. Sato, T. Ishii, S. Isakosawa, and K. Shii, *Formations of rhombohedral boron nitride, as revealed by TEM-electron energy loss spectroscopy*, J. Mater. Sci. 16 (1981), pp. 1114–1116.

[3] R.H. Wentorf, Jr., *Synthesis of the cubic form of boron nitride*, J. Chem. Phys. 34 (1961), pp. 809–812.
[4] F.P. Bundy and R.H. Wentorf, Jr., *Direct transformation of hexagonal boron nitride to denser forms*, J. Chem. Phys. 38 (1963), pp. 1144–1149.
[5] V.I. Levitas, J. Hashemi, and Y.Z. Ma, Strain-induced disorder and phase transformation in hexagonal boron nitride under quasi-homogeneous pressure: In situ X-ray study in a rotational diamond anvil cell, *Europhys Lett.* 68 (2004), pp. 550–556.
[6] F.R. Corrigan and F.P. Bundy, *Direct transitions among the allotropic forms of boron nitride at high pressures and temperatures*, J. Chem. Phys. 63 (1975), pp. 3812–3820.
[7] V.F. Britun and A.V. Kurdyumov, *Mechanisms of martensitic transformations in boron nitride and conditions of their development*, High Press. Res. 17 (2000), pp. 101–111.
[8] T. Taniguchi, T. Sato, W. Utsumi, T. Kikegawa, and O. Shimomura, *Effect of non-hydrostaticity on the pressure induced phase transformation of rhombohedral boron nitride*, Appl. Phys. Lett. 70 (1997), pp. 2392–2394.
[9] V.L. Solozhenko and F. Elf, *On the threshold pressure of the hBN-to-wBN phase transformation at room temperature*, J. Superhard. Mater. 20 (1998), pp. 62–63.
[10] N. Dubrovinskaia, V.L. Solozhenko, N. Miyajima, V. Dmitriev, O.O. Kurakevych, and L. Dubrovinsky, *Superhard nanocomposite of dense polymorphs of boron nitride: Noncarbon material has reached diamond hardness*, Appl. Phys. Lett. 90 (2007), pp. 101912–101914.
[11] V.L. Solozhenko, G. Will, and F.J. Elf, *The equation of state of hexagonal graphite-like boron nitride to 12 GPa and phase transformation hBN to wBN*, Annual Report 1995, Hamburger Synchrotronstrahlungslabor (HASYLAB), Hamburg, Germany, Pt 2, p. 507, 1996.
[12] V.I. Levitas, Y. Ma, J. Hashemi, M. Holtz, and N. Guven, *Strain-induced disorder, phase transformations, and transformation-induced plasticity in hexagonal boron nitride under compression and shear in a rotational diamond anvil cell: In situ X-ray diffraction study and modeling*, J. Chem. Phys. 125 (2006), pp. 044507–044520.
[13] Y. Meng, H.K. Mao, P.J. Eng, T.P. Trainor, M. Newville, M.Y. Hu, C. Kao, J. Shu, D. Hausermann, and R.J. Hemley, *The formation of sp3 bonding in compressed BN*, Nat. Mater. 3 (2004), pp. 111–114.
[14] S.N. Dub and I.A. Petrusha, *Mechanical properties of polycrystalline cBN obtained from pyrolytic gBN by direct transformation technique*, High Press. Res. 26 (2006), pp. 71–77.
[15] T. Taniguchi, T. Sato, W. Utsumi, T. Kikegawa, and O. Shimomura, *In-situ X-ray observation of phase transformation of rhombohedral boron nitride under static high pressure and high temperature*, Diamond Relat. Mater. 6 (1997), pp. 1806–1815.
[16] H. Lorenz and I. Orgzall, *Influence of the initial crystallinity on the high pressure–high temperature phase transition in boron nitride*, Acta Mater. 52 (2004), pp. 1909–1916.
[17] V.F. Britun, A.V. Kurdyumov, N.I. Borimchuk, V.V. Yarosh, and A.I. Danilenko, *Formation of diamond-like BN phases under shock compression of graphite-like BN with different degree of structural ordering*, Diamond Relat. Mater. 16 (2007), pp. 267–276.
[18] L.C. Nistor, G. Van Tendeloo, and G. Dinca, *Crystallographic aspects related to the high pressure–high temperature phase transformation of boron nitride*, Philos. Mag. 85 (2005), pp. 1145–1158.
[19] A.V. Kurdyumov, V.F. Britun, and I.A. Petrusha, *Structural mechanisms of rhombohedral BN transformations into diamond-like phases*, Diamond Relat. Mater. 5 (1996), pp. 1229–1235.
[20] C. He, L. Sun, C. Zhang, X. Peng, K. Zhang, and J. Zhong, *Z-BN: A novel superhard boron nitride phase*, Phys. Chem. Chem. Phys. 14 (2012), pp. 10967–10971.
[21] C. Jiang, J. Zhao, and R. Ahuja, *A novel superhard BN allotrope under cold compression of h-BN*, J. Phys. Condens. Matter. 25 (2013), pp. 122204–122209.
[22] L. Hromadová and R. Martoňák, *Pressure-induced structural transitions in BN from ab initio metadynamics*, Phys. Rev. B 84 (2011), pp. 224108–224114.
[23] S. Zhang, Q. Wang, Y. Kawazoe, and P. Jena, Three-dimensional metallic boron nitride, J. Am. Chem. Soc. 135 (2013), pp. 18216–18221.
[24] T. Taniguchi, K. Kimoto, M. Tansho, S. Horiuchi, and S. Yamaoka, Phase transformation of amorphous boron nitride under high pressure, Chem. Mater. 15 (2003), pp. 2744–2751.

[25] B.P. Singh, G. Nover, and G. Will, *High pressure phase transformations of cubic boron nitride from amorphous boron nitride using magnesium boron nitride as the catalyst*, J. Cryst. Growth 152 (1995), pp. 143–149.
[26] J.Y. Huang and Y.T. Zhu, Atomic-scale structural investigations on the nucleation of cubic boron nitride from amorphous boron nitride under high pressures and temperatures, Chem. Mater. 14 (2002), pp. 1873–1878.
[27] H. Lorenz and I. Orgzall, *In situ observation of the crystallization of amorphous boron nitride at high pressures and temperatures*, Scr. Mater. 52 (2005), pp. 537–540.
[28] V.L. Solozhenko and E.G. Solozhenko, *Equation of state of turbostratic boron nitride*, High Press. Res. 21 (2001), pp. 115–120.
[29] V.L. Solozhenko, O.O. Kurakevych, and Y.L. Le Godec, *Creation of nanostuctures by extreme conditions: high-pressure synthesis of ultrahard nanocrystalline cubic boron nitride*, Adv. Mater. 24 (2012), pp. 1540–1544.
[30] V.L. Solozhenko and O.O. Kurakevych, *Reversible pressure-induced structure changes in turbostratic BN–C solid solutions*, Acta Crystallogr. B 61 (2005), pp. 498–503.
[31] V.L. Solozhenko, O.O. Kurakevych, and A.Y. Kuznetsov, *Raman scattering from turbostratic graphitelike BC4 under pressure*, J. Appl. Phys. 102 (2007), pp. 063509–063513.
[32] T. Kobayashi, S. Tashiro, T. Sekine, and T. Sato, Phase transformation of turbostratic BN by shock compression, Chem. Mater. 9 (1997), pp. 233–236.
[33] M.C. Wilding, M. Wilson, and P.F. McMillan, *Structural studies and polymorphism in amorphous solids and liquids at high pressure*, Chem. Soc. Rev. 35 (2006), pp. 964–986.
[34] A.R. Yavari, *Metallic glasses: The changing faces of disorder*, Nat. Mater. 6 (2007), pp. 181–182.
[35] P. Ordejón, E. Artacho, and J.M. Soler, *Self-consistent order-N density-functional calculations for very large systems*, Phys. Rev. B 53 (1996), pp. R10441–R10444.
[36] M. Durandurdu, *Hexagonal nanosheets in amorphous BN: A first principles study*, J. Non-Cryst. Solids. 427 (2015), pp. 41–45.
[37] R. Zedlitz, M. Heintze, and M.B. Schubert, *Properties of amorphous boron nitride thin films*, J. Non-Cryst. Solids. 198 (1996), pp. 403–406.
[38] J.Y. Huang, H. Yasuda, and H. Mori, *HRTEM and EELS studies on the amorphization of hexagonal boron nitride induced by ball milling*, J. Am. Ceram. Soc. 83 (2000), pp. 403–409.
[39] N. Troullier and J.M. Martins, *Efficient pseudopotentials for plane-wave calculations*, Phys. Rev. B 43 (1991), pp. 1993–2006.
[40] A.D. Becke, *Density-functional exchange energy approximation with correct asymptotic behavior*, Phys. Rev. A 38 (1988), pp. 3098–3100.
[41] C. Lee, W. Yang, and R.G. Parr, Development of the Colle-Salvetti correlation-energy formula into a functional of the electron density, Phys. Rev. B 37 (1988), pp. 785–789.
[42] M. Parrinello and A. Rahman, *Polymorphic transitions in single crystals: A new molecular dynamics method*, J. Appl. Phys. 52 (1981), pp. 7182–7190.
[43] Y.K. Park, *Molecular-dynamics study of defect formation in hydrogenated amorphous silicon*, Ph.D. diss., *Texas Tech University*, Lubbock, TX, 1994.
[44] C.W. Myles, B.C. Ha, and Y.K. Park, *Large supercell molecular dynamics study of defect formation in hydrogenated amorphous silicon*, J. Phys. Chem. Solids 63 (2002), pp. 1691–1698.
[45] Siesta manual (3.2) p. 85, http://departments.icmab.es/leem/siesta/Documentation/Manuals
[46] H.J. Monkhorst, J.D. Pack, *Special points for Brillouin-zone integrations*, Phys. Rev. B 13 (1976), pp. 5188–5192.
[47] S. Le Roux and V. Petkov, *ISAACS-interactive structure analysis of amorphous and crystalline systems*, J. Appl. Crystallogr. 43 (2010), pp. 81–85.
[48] K. Momma and F. Izumi, *VESTA 3 for three-dimensional visualization of crystal, volumetric and morphology data*, J. Appl. Crystallogr. 44 (2011), pp. 1272–1276.
[49] Y. Kumashiro (ed.), *Electric Refractory Materials*, Taylor & Francis, New York, NY, 2000.
[50] H.S. Wu, X. Hong Xu, F.Q. Zhang, and H. Jiao, *New boron nitride B24N24 nanotube*, J. Phys. Chem. A 107 (2003), pp. 6609–6612.
[51] H.-S. Wu and H. Jiao, *What is the most stable B24N24 fullerene?*, Chem. Phys. Lett. 386 (2004), pp. 369–372.